ORIGINAL ARTICLE

Development of an SO$_2$ indicator label applied to shrimp

Gleyca de Jesus Costa Fernandes[1] , Karoline Ferreira Silva[1] , Clara Suprani Marques[2] ,
Luiza Zazini Benedito[1] , Beatriz Ribeiro Cabral[3] , Pedro Henrique Campelo[2] ,
Soraia Vilela Borges[3] , José Manoel Marconcini[4] , Zuy Maria Magriotis[5] , Pedro Ivo Cunha Claro[6]
and Marali Vilela Dias[3]*

[1]Departamento de Ciências Florestais, Universidade Federal de Lavras, Lavras, MG, Brasil
[2]Departamento de Tecnologia de Alimentos, Universidade Federal de Viçosa, Viçosa, MG, Brasil
[3]Departamento de Ciência de Alimentos, Universidade Federal de Lavras, Lavras, MG, Brasil
[4]Embrapa Instrumentação, São Carlos, SP, Brasil
[5]Departamento de Engenharia, Universidade Federal de Lavras, Lavras, MG, Brasil
[6]Departamento de Engenharia de Materiais, Universidade Federal de São Carlos, São Carlos, SP, Brasil
*maraliileladias@gmail.com

Abstract

Sulfiting agents are added to crustaceans products to prolong their shelf life. However, depending on the concentration, these agents can be toxic to consumers due to the presence of SO$_2$. In this context, a colorimetric indicator label based on starch and iodine was developed to detect SO$_2$ in shrimp, showing whether the product is safe or not for consumers. The incorporation of iodine into the starch matrix resulted in labels with a smooth and homogeneous surface, and reduced water solubility from 9.26% to around 0.12%. In both *in vitro* and shrimp paste test, a visual detection response was observed in the label containing 0.02% of iodine when evaluated in the presence of 100 to 160 ppm of SO$_2$, with ΔE^* values greater than 5 (can be identifiable by the human eye). Therefore, the elaborated label showed potential as an economical and simple method to detect SO$_2$ concentration in shrimp-based foods.

Keywords: *colorimetric indicator, crustaceans, food safety, smart label.*

1. Introduction

Crustaceans are highly perishable foods due to their high contents of amino acids, moisture, and their microbiota composition. Therefore, their shelf life depends on the processing techniques, additives, packaging technology, and storage conditions[1]. Sulfiting agents are the most commonly used preservatives aiming at extending the product shelf life, preventing color changes among other functions. However, their main residue, sulfur dioxide (SO$_2$), can cause allergic reactions and asthma attacks in humans when at high concentrations[2].

In Brazil, the National Health Surveillance Agency (ANVISA) is responsible for regulating the use of several active ingredients in food, supported by Resolution nº 329/2019, which establishes a maximum residual concentration of SO$_2$ of 100 ppm in frozen or chilled crustacean, and 150 ppm in ready-to-eat seafood[3]. Concentrations exceeding these limits can negatively affect consumers, food handlers, and buyers/importers[4]. Several methods are used to determine the SO$_2$ concentration in foods, such as volumetric titration, rapid test with strips of paper, and more accurate and powerful techniques, as high-performance liquid chromatography[5]. However, these methods have some disadvantages, including

the high cost of reagents, instrumental infrastructure, and long analysis times. A possible innovative and low-cost alternative to ensure the safe consumption of crustaceans could be a smart packaging composed of a colorimetric indicator system[6,7].

Smart or intelligent packaging conveys information to consumers/handlers about the presence of certain substances in the product, such as gases, for example, and it is a novel strategy that could result in benefits for the seafood industry[7,8]. Indicator labels are better options than other detection methods since they are easy to apply and understand (based on color changes), in addition to providing quick and reliable results[8]. Also, they could bring advantages for the consumers regarding food safety.

Recently, a few studies regarding the development of optical sensors and indicators systems of SO$_2$ in food products have been conducted. Bener et al.[6] elaborated a potential sensitive optical sensor for SO$_2$ detection in food matrices. Fu et al.[9], in turn, manufactured a smart PET/paper chip platform for detecting SO2 in food based on microfluidic device and color change by acid-basic indicator. At last,

Fernandes, G. J. C., Silva, K. F., Marques, C. S., Benedito, L. Z., Cabral, B. R., Campelo, P. H., Borges, S. V., Marconcini, J. M., Magriotis, Z. M., Claro, P. I. C., & Dias, M. V.

Khamkhajorn et al.[10] developed a colorimetric-based method to SO_2 detection through a smartphone software.

In this context, the present study aimed to develop and characterize a colorimetric indicator starch-based label incorporated with iodine to detect SO_2 in a shrimp paste. It was investigated the hypothesis that the manufactured label would change color when in contact with sulfite-containing foods, enabling an easy and quick detection of high concentrations of SO_2. To allow the preparation of this kind of label, this study was based on the Landolt reaction, which explains the starch/iodine/sulfite interaction[11].

2. Materials and Methods

2.1 Materials

The experimental labels were elaborated from cassava 406 starch (Indústria Agro Comercial Cassava SA, Brazil). According to the manufacturer, the starch was previously modified by esterification. Resublimed iodine (Exôdo Científica, Brazil); potassium iodide (Proquimios, Brazil); and sodium metabisulfite (Exodus Científica, Brazil) were also used. The shrimp paste was made from peeled and frozen southern brown shrimp (*Farfantepenaeus subtilis*) acquired from a local market.

2.2 Experimental design

A sequential design was used, in which the smart labels were developed with two iodine concentrations and characterized. Subsequentialy, the best-performing label was tested *in vitro* by contact with solutions with different SO_2 concentrations, at 4 °C, simulating a cold storage condition, and in contact with a shrimp paste that contained SO_2 concentrations ranging from 100 to 120 ppm. The design was completely randomized with three replicates.

2.3 Labels preparation

Starch was dispersed in deionized water, following the proportion of 3% (wt/v), under heating and magnetic stirring at 70 °C for 15 min. Subsequently, the dispersions were cooled down to approximately 30 °C, and iodine (I_2) and potassium iodide (KI) were added and homogenized[12]. The samples were named FI2 (0.02% wt/v of I_2 and 0.04% wt/v of KI) and FI4 (0.04% wt/v of I_2 and 0.08% wt/v of KI). After complete solubilization of I_2, the labels were obtained by the casting method, in which 20 g of the dispersions were poured into plastic Petri dishes (Ø = 85 mm) and left on a bench at approximately 25 °C until solvent evaporation (about 18 h). After drying, the labels were removed from the dishes and stored at 23 °C ± 2 °C and 50% ± 5% relative humidity until analysis. A control label with starch only (PS) was manufactured for comparision purposes.

2.4 Characterization techniques

Fourier transform infrared spectroscopy in attenuated total reflectance (FTIR-ATR, Vertex 70, Bruker, USA), with a zinc selenide crystal, was performed to evaluate the interactions between iodine and the starch matrix. The spectra were obtained with 32 scans per sample at a resolution of 2 cm^{-1} in the 400 to 4000 cm^{-1} range.

Micrographs of cross-sections of the samples were taken to evaluate the morphology and homogeneity of the labels. The samples were fixed on stubs with double-sided carbon tape and were sputtered with gold to increase their conductivity. The samples were observed in a scanning electron microscope coupled with energy dispersive x-ray (SEM-EDS, JSM 6510, JEOL, Japan) with an electron acceleration voltage of 10 kV. The EDS method coupled to SEM was used to determine the qualitative composition and map the iodine distribution in the starch matrix. The parameters adopted for this analysis were a voltage of 15 kV and a mapping time of 45 min. In the EDS maps, the intensity of the points indicated the component concentration, and the colors pink, green, and blue corresponded to oxygen, carbon, and iodine, respectively.

The solubility of the films was evaluated to determine their water resistance since their intended application was on high-moisture products. For this purpose, the films were weighed and immersed in 100 mL of distilled water for 24 h. After, the water was drained, and the films were dried in an oven at 105 °C for 24 h and then weighed[13]. Finally, the portion of the films solubilized in water was calculated according to Equation 1:

$$\%SM = \frac{\left[\left(w_i - w_f\right).100\right]}{w_i} \quad (1)$$

in which %SM is the percentage of solubilized material; w_i is the initial weight of the sample; and w_f is the final weight of the sample after drying.

Thermogravimetry analysis (TGA) was performed in a Shimadzu TGA-50 thermogravimetric analyzer (Japan). Approximately 7 mg of material was heated at a rate of 10 °C.min^{-1} in a nitrogen atmosphere (50 mL.min^{-1}) from 25 °C to 800 °C. This analysis was performed to evaluate whether the incorporation of iodine would produce changes in the thermal decomposition behavior of the labels and determine the materials' degradation temperature, which was necessary for performing the differential scanning calorimetry (DSC) analysis.

The thermal analyses by DSC were performed in a Shimadzu DSC TA 60 thermal analyzer (Japan). Heating and cooling ramps were performed at a rate of 10 °C.min^{-1} in a nitrogen atmosphere, in which the temperature varied between -50 °C and 200 °C. By knowing the glass transition temperature (T_g) of the film, it was possible to predict the label behavior under temperature change in specific applications[14].

The color of the labels was instrumentally determined in a Konica Minolta CM-5 colorimeter (Japan) using the CIELAB system, D65 illuminant, standard 10° observer angle, and reflectance mode. The colorimetric coordinates were analyzed and calculated according to Luchese et al.[15], describing the luminosity (L*), which ranges from 0 (light tones) to 100 (dark tones); the coordinate a* (variation in the color space from green (-a) to red (+a)); and the coordinate b* (variation in the color space from blue (-b) to yellow (+ b)). In this color space, C* represents chroma or saturation, and its value is the distance from the luminosity axis (L*), starting at 0 in the center. The hue angle (h*) begins on the

+a* axis and moves counterclockwise; along this path, values close to 0° represent red, close to 90° represent yellow, close to 180° represent green, and close to 270° represent blue.

2.5 In vitro evaluation of the label

The label that performed best in the characterization analyses was exposed to SO_2 solutions at different concentrations (40 to 200 ppm, with 20-ppm intervals), at 4 °C for 15 min. After, the labels were dried, and the color analysis was performed. The L* and h* parameters were evaluated as described in section 2.4 to monitor the color change after contact with the SO_2 solutions. The total difference (ΔE^*) was calculated by the sum of differences in the L*, a*, and b* values before versus after contact with the different SO_2 solutions (Equation 2):

$$\Delta E^* = \left[\left(\Delta L^* \right)^2 + \left(\Delta a^* \right)^2 + \left(\Delta b^* \right)^2 \right]^{1/2} \qquad (2)$$

2.6 Application on a shrimp-based product

The manufactured labels were tested on a shrimp-based product. Since commercial shrimp already contain sulfite, the acquired samples were previously immersed in distilled water for 20 min and washed twice to reduce the remaining sulfite present. Then, sodium metabisulfite ($Na_2S_2O_5$) was applied in the shrimps to reach the final desired concentrations of 100, 110 and 120 ppm. Subsequently, 50 g of shrimp was ground to a paste and stored at 4 ± 2 ºC in the presence of the indicator labels. An illustrative scheme of the labels is displayed in Figure 1.

To ensure that the concentrations of 100, 110 and 120 ppm were achieved, iodometric titration without heating was performed as follow[16]: 10 mL of sample solution was transferred to an Erlenmeyer flask, and then 1.4 mL of hydrochloric acid (1 mol.L⁻¹) and 1 mL of 1% (wt./v) starch solution were added. Titration was performed with iodine and N/63 bicarbonate until the solution turned blue. The SO_2 concentration in ppm was obtained using the Equation 3:

$$c_{SO_2} = \frac{5000 \; V}{W} \qquad (3)$$

in which C_{SO2} is the residual SO_2 concentration (ppm), V is the volume (mL) spent in the titration with N/63 bicarbonate solution and iodine, and W is the weight (g) of the sample.

Regarding the blank, even after the washing steps, it was not possible to obtain a sample without any SO_2, so the reference sample was made from shrimp without the addition of $Na_2S_2O_5$, which had a residual SO_2 concentration of 80 ppm.

2.7 Color and transparency analysis of the labels

The colorimetric variations of the indicator labels exposed to the shrimp samples at different SO_2 concentrations (100, 110, and 120 ppm) were measured by analyzing the L*, C*, and h* coordinates (Section 2.4). The ΔE^* parameter was obtained as described in section 2.5.

The transparency of the films, which indicates the films' loss of color, was measured with a GBC UV/VIS 918 spectrophotometer (Shimadzu, Tokyo, Japan) according to ASTM D1746-15[17], by measuring the percentage of transmittance (%T) at 600 nm. The transparency (T600) was calculated according to Equation 4, where δ is the film thickness (mm):
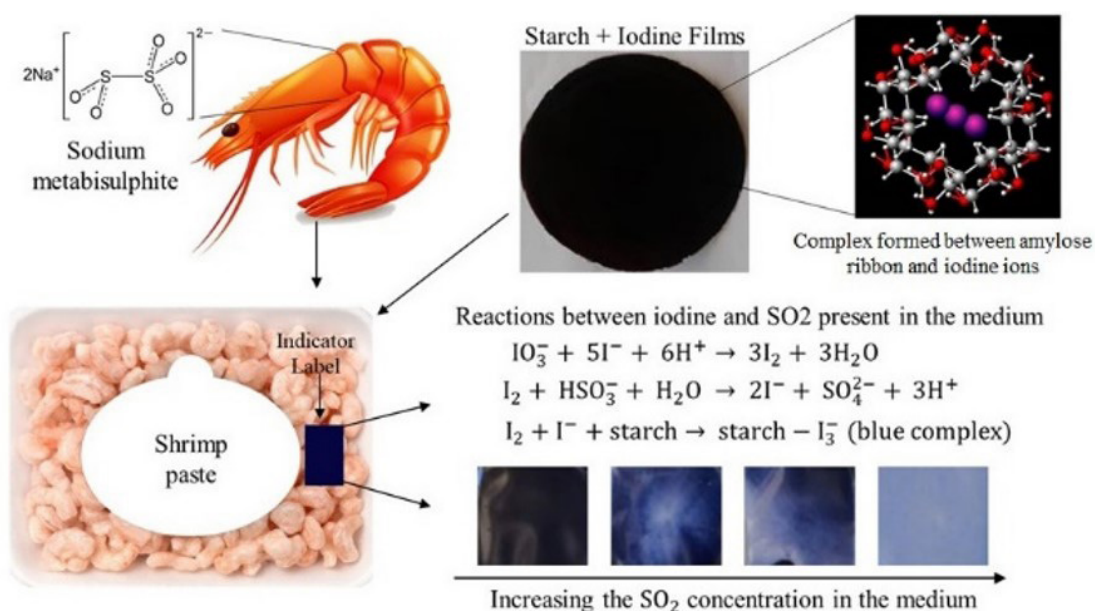
Figure 1. A schematic depiction of the indicator label's application as smart packaging and the chemical reactions that occur.

$$T_{600} = \frac{\text{Log \%T}}{\delta} \qquad (4)$$

2.8 Statistical analysis

Water solubility, color (L*, a*, b*, C*, h*, and ΔE*), and transparency data were subjected to analysis of variance (ANOVA), and the treatment means were compared using Tukey's test at 5% probability, when deemed appropriate. The statistical analyses were performed in Statistica 8.0 (StatSoft, Dell, USA). The FTIR, TGA, DSC, SEM, and EDS data were subjected to descriptive analysis.

3. Results and Discussions

3.1 Labels characterization

The FTIR spectra obtained for all samples are displayed in Figure 2. The pure starch label (PS) spectrum presented characteristic bands at 3294 cm^{-1}, 2925 cm^{-1}, and 1641 cm^{-1}, corresponding to stretching of the OH bonds of starch, and stretching of the CH and OH bonds of the water present in the starch matrix, respectively[18]. By incorporating iodine into the polymer matrix, the band at 3294 cm^{-1} shifted to 3288 cm^{-1}, possibly due to the interaction between the iodine molecules with starch. The FTIR spectra in the 3500-3200 cm^{-1} range can indicate the hydrophobicity of biopolymers[18]. Therefore, the displacement of the signal to a region of lower energy may mean fewer starch interactions with water, which means the films with iodine would be more hydrophobic[19].
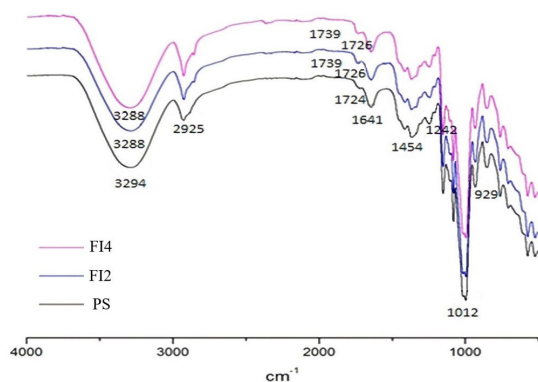
Figure 2. FTIR spectra of the manufactured starch labels: with 0.02% of iodine (FI2), with 0.04% of iodine (FI4), and a control without iodine (PS).

The obtained cross-section-micrographs are displayed in Figure 3. All starch labels, with and without the addition of iodine, were compact, with a smooth and homogeneous surface, possible indicating good interaction and compatibility between the components..

The Figure 4 shows the EDS maps with the main elements present in the labels. Carbon (C) and oxygen (O) are represented in the images by pink and green dots, respectively, and are highly abundant because starch consists mostly of these elements. Regarding iodine (blue), FI4 had a higher intensity of dots, confirming the higher concentration of this element in this label when compared to FI2. Overall, the distribution of iodine in the matrix was homogeneous in both formulations, which is important to allow a colorimetric response of the same intensity in any label region, ensuring its efficacy.

Regarding the solubility of the films, the obtained results are displayed in Table 1. The films solubility in water is closely related to the interactions of their components[20]. Starch labels usually show high water solubility at 25 °C due to the hydroxyl groups present in their structure[21,22]. The low water solubility of iodine impacted the solubility of the labels when compared to the control, reducing it by almost 75 times. When compared to each other, however, no significant difference was verified between FI2 and FI4. As observed in the FTIR spectra (Figure 2), the addition of iodine to the starch matrix led to a decrease in the free OH groups when compared to the control sample, consequently reducing the water solubility of the labels. The FTIR spectra obtained for FI2 and FI4, on the other hand, were quite similar, suggesting that the effect on water solubility of the starch labels depended more on iodine presence rather than its concentration. This factor favored an increase in the stability of the labels, allowing them to remain intact even when submerged in water for 24 h, which is an attractive property for application in foods with high moisture content.

The thermal analyses results can be observed in Figure 5.

Table 1. Water solubility values of the manufactured indicator labels.

Treatment	Solubility (%)
PS	9.258 ± 0.005[b]
FI2	0.127 ± 0.007[a]
FI4	0.112 ± 0.009[a]

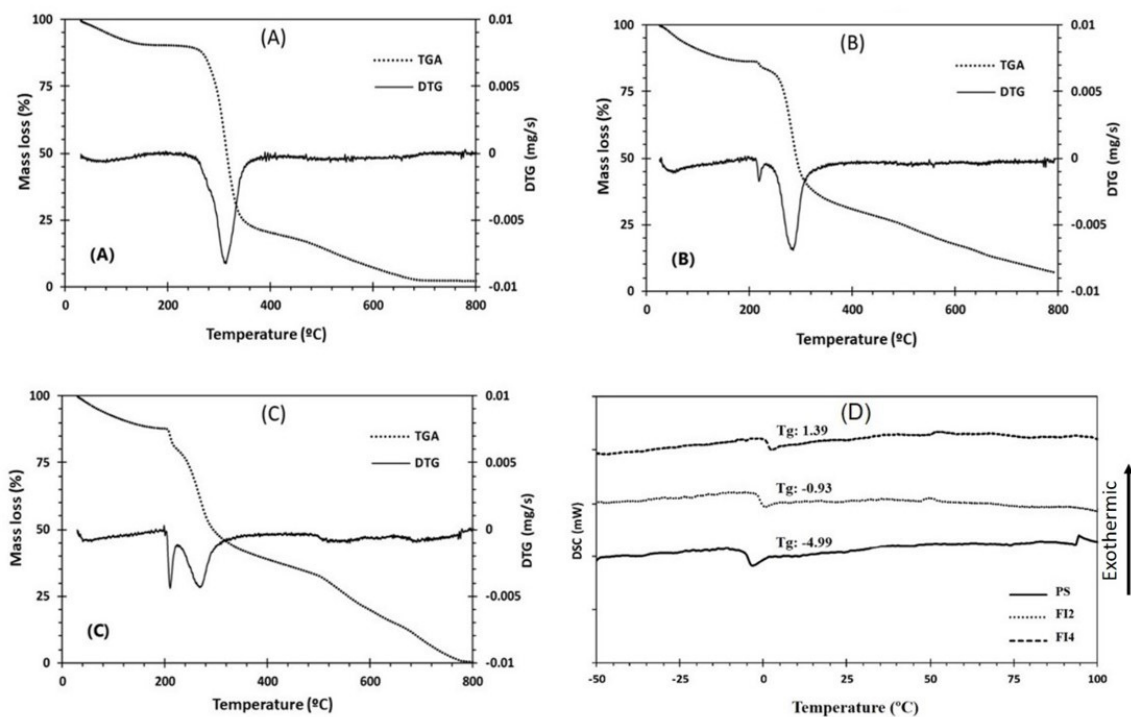PS - pure starch; FI2 (0.02% I_2 and 0.04% KI); FI4 (0.04% I_2 and 0.08% KI). Means followed by different letters in the column are significantly different by Tukey's test (p<0.05).
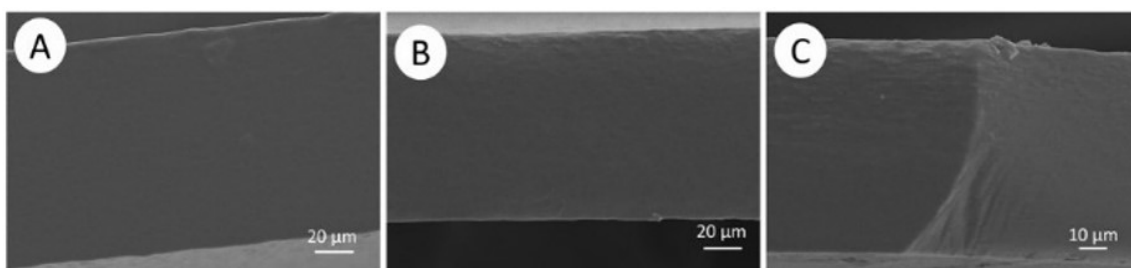
Figure 3. Cross-sectional photomicrographs: (A) control film; (B) FI2 (0.02% I_2 and 0.04% KI); and (C) FI4 (0.04% I_2 and 0.08% KI).
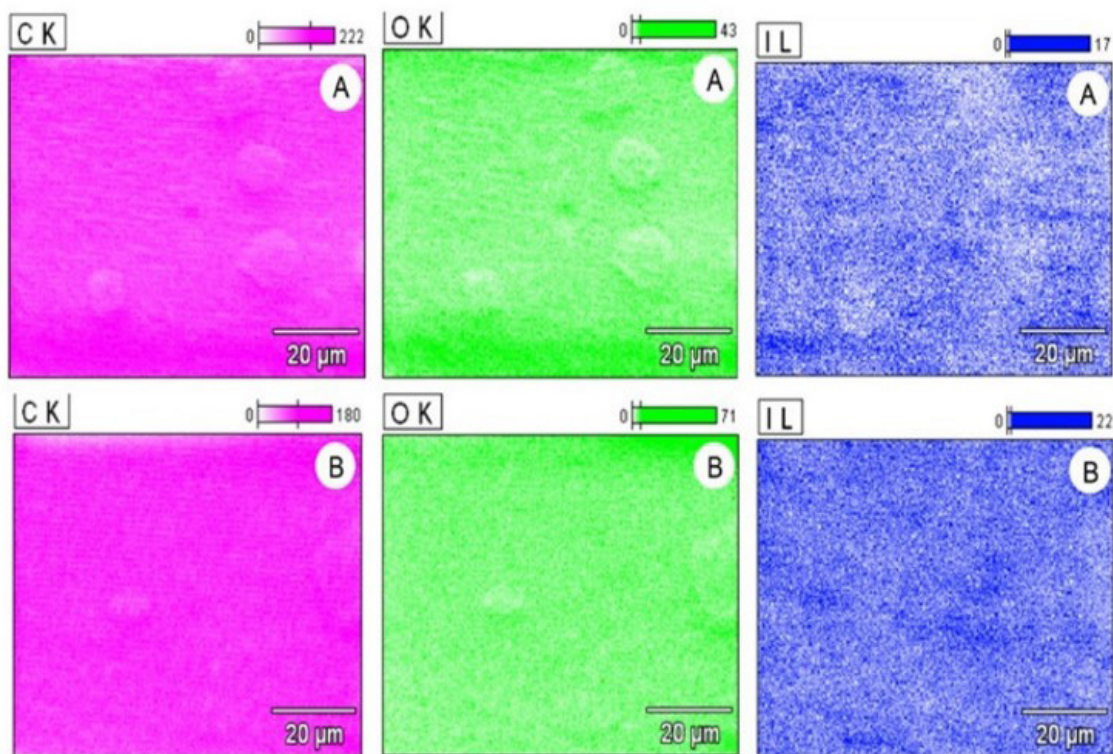
Figure 4. EDS images of the indicator labels: (A) FI2 (0.02% I$_2$ and 0.04% KI) and (B) FI4 (0.04% I$_2$ and 0.08%KI). Carbon: pink; oxygen: green; iodine: blue.

Figure 5. Thermogravimetric (TG) and differential thermogravimetric (DTG) curves for (A) pure starch label(PS, control); (B) FI2 (0.02% I$_2$ and 0.04% KI); and (C) FI4 (0.04% I2 and 0.08% KI); (D) DCS curves for PS, FI2, and FI4 labels.

The PS TG curve (Figure 5A) showed mass loss in three stages, while FI2 and FI4 TG curves (Figure 5B and 5C, respectively) showed mass losses in four different stages. The first stage observed for all samples was attributed to water loss[23]. Regarding the PS labels, the second stage (265-453 °C) was related to the thermal degradation of amylose and amylopectin, with a mass loss around 69%.

Concerning FI2 and FI4, the second stage of mass change (200-240 ºC) was related to the sublimation of the iodine[24]. After this event, there was thermal decomposition of starch. With the addition of iodine, the maximum degradation temperature of the label decreased from 310 °C in the control film to 280 °C and 270 °C in FI2 and FI4, respectively. This was most likely due to electrostatic interactions between I_3^- and the carbonyl groups present in starch[24]. It was observed that the increase in iodine concentration from 0.02% to 0.04% slightly reduced the thermal stability of the labels. Similar behavior was observed by Chen et al.[25] when investigating carboxymethyl chitosan films grafted with iodine. Regarding the residual mass, there was an increase in the percentage of residues as the iodine concentration in the matrix increased: it went from 15.4% in PS to 20.3% in FI2 and 34.82% in FI4. Since the starch concentration was not changed, this increase may be related to the potassium and iodine added to the medium[24,26].

The DSC curves (Figure 5D) showed that the incorporation of iodine in the matrix, as well as the increase in its concentration, increased the samples' glass transition temperature (T_g). This was probably due to a higher amount of energy required for chain mobility in the polymer as a consequence of the interactions between iodine and the starch matrix, through dipolar force. The iodine incorporated forms complexes with the amylose fraction of the starch, resulting in films with a dark blue color (Figure 1). It is discussed that the entering of iodine into the helical structure of amylose makes it stiffer and probably alters T_g[27]. Thus, the higher T_g value of the FI4 label may be related to the higher iodine concentration[28].

For all treatments, the T_g values were close to 0 °C, indicating that, at the recommended temperature for fresh shrimp storage (between 0 ºC and 4 ºC), the films would be above their T_g. In this temperature range, it would be expected a greater malleability of the polymer chains since they are in the elastomeric state[29]. This feature is important to the labels' performance since it enables their accommodation on the irregular surface of the shrimp . In this sense, it is noteworthy to mention that storage temperatures below 0 ºC (more specifically, below the T_g) would not be ideal for the developed labels, since the materials would become more rigid, stiff, and brittle, compromising their use.

Concerning the color analysis, the increase in iodine concentration did not influence (p>0.05) the L*, a*, b*, or C* coordinates (Table 2). The coordinates a* and b* remained negative, indicating the predominance of blue and green color; the luminosity (L*) did not decrease, and the saturation (C*) did not increase significantly. Concerning h*, it did change significantly; however, the obtained values remained in the range between 200 and 295 º, representing a predominance of the color blue[30].

3.2 In vitro and in shrimp paste tests

According to the characterization results, the higher iodine concentration did not increase thermal stability nor decrease water solubility; regarding the color analysis, it only influenced h*, which remained within the blue range in both formulations. Therefore, a higher iodine concentration in the label was not attractive for application, and the following tests were performed only with the FI2 label. Besides that, taking into account that migration of iodine to the food could occur, labels with a smaller concentration of the substance would be preferable. The recommended intake of iodine is 150 µg/day for adults, however, it is known that, with the exception of susceptible individuals, exposure to higher doses are usually well tolerated[31]. Although iodine migration to food was not investigated in the present work, it would be interesting to verify if it could indeed occur and if the it would pose a risk to consumers.
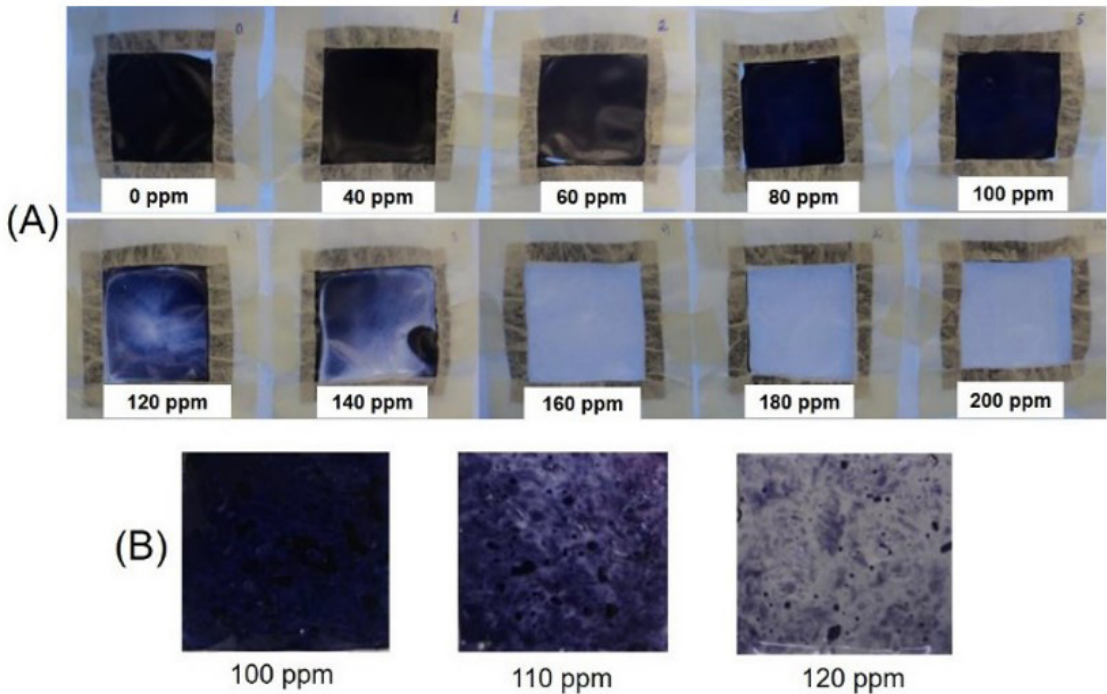
When in contact with solutions with different SO_2 concentrations, the L*, h*, and ΔE* values of FI2 label changed (Figure 6A). Higher SO_2 concentrations promoted an increase in L* values and a reduction in the blue hue (h*), resulting in lighter and even transparent labels. The ΔE* values were satisfactory for a 120 to 160 ppm concentration range. Concentrations of SO_2 greater than 120 ppm led to ΔE* values greater than 5, a change that can be identifiable by the human eye[30]. For SO_2 concentrations above 160 ppm, the ΔE* values were above 12, which implies an absolute color difference, i.e., there was total discoloration of the labels, allowing visual identification when the SO_2 in the product is higher than the limit allowed by Brazilian legislation for ready-to-eat seafoods (150 ppm)[3].

In this case, the increase in the SO_2 concentration caused a more significant discoloration, which is explained by the Landolt reaction but in reverse. In this reaction, a potassium iodate (KIO_3) solution is added to an acidified sodium bisulfite ($NaHSO_3$) solution containing starch. The iodate (IO_3^-) is oxidized to iodine (I_2), but in the presence of bisulfite (HSO_3^-), it rapidly reduces to iodate (IO_3^-) again, keeping the medium colorless. After that, when all the bisulfite in the system is consumed, it leads to the accumulation of iodine and a complex distribution of $^-$ and I_5^-, which reacts with starch, changing the system color to dark blue (Figure 1)[9]. For the labels developed in this study, the bisulfite in the

Table 2. Color coordinates of the manufactured labels.

Treatment	L*	a*	b*	C*	h*
FI2	20.24±0.97[a]	-0.04±0.04[a]	-0.36±0.22[a]	0.36±0.22[a]	263.04±2.89[b]
FI4	17.56±1.63[a]	-0.14±0.09[a]	-0.50±0.27[a]	0.52±0.29[a]	255.07±3.41[a]

FI2 (0.02% I_2 and 0.04% KI); FI4 (0.04% I_2 and 0.08% KI). Means followed by different letters in the same column are significantly different (ANOVA) (p<0.05).

Figure 6. (A) FI2 label after contact with different SO$_2$ solutions at 4 °C and (B) after contact with shrimp paste.

Table 3. Color and transparency parameters of the indicator label (FI2) applied to shrimp.

Coordinates	SO$_2$ (ppm)		
	100	110	120
L*	23.60 ± 0.18 [c]	28.82 ± 0.29 [b]	32.71 ± 0.19 [a]
h*	38.48 ± 5.08 [a]	40.83 ± 3.10 [a]	30.77 ± 8.61 [a]
ΔE*	3.58 ± 1.13 [c]	8.68 ± 0.78 [b]	12.49 ± 0.88 [a]
C*	0.94 ± 0.03[a]	0.99 ± 0.06[a]	0.38 ± 0.04[b]

Means followed by different letters, in the same row, are significantly different by Tukey's test ($p < 0.05$).

medium reacted with the iodine–amylose complex, leading to the discoloration of the dark-blue color of the matrix.

For concentrations up to 100 ppm, the ΔE* values were lower than the limit of perception of the human eye (ΔE*<5), which would not affect the application of the labels when used in chilled crustaceans. However, new tests would be needed for application in other markets with more flexible laws. Nevertheless, the good performance of the discoloration rate of the label in the *in vitro* test demonstrated its suitability for testing on food.

Among the color coordinates, those significantly affected ($p < 0.05$) by variations in the SO$_2$ concentration when the label was applied to the shrimp paste were L*, C*, and ΔE* (Table 3). SO$_2$ concentrations in shrimp paste greater than 120 ppm caused an increase in L* and a decrease in C* in the labels, resulting in lighter and less saturated labels, i.e., loss of color after contact with the shrimp paste. The h* coordinate did not differ significantly between the samples

as a function of the SO$_2$ concentration, meaning there was a similar hue.

The ΔE* parameter increased significantly with the SO$_2$ concentration. In the samples exposed to 110 ppm and 120 ppm, the ΔE* values were greater than 5, indicating easy detection by the human eye (Figure 6B). In this case, the determination of ΔE* becomes extremely important, as products that were not in accordance with the most restrictive legislation (100 ppm) would be easily perceived by the human eye if the label FI2 was used.

4. Conclusion

The incorporation of 0.02% of iodine into the starch matrix reduced the water solubility of the elaborated labels and increased their thermal stability. The tests *in vitro* and in shrimp paste showed that the labels have potential for use as a colorimetric indicator system to help verify the residual SO$_2$ concentration in shrimp. Due to the simplicity of this system, easy production, and low cost, these labels may find application in the seafood industry to inspect the SO$_2$ concentration in crustaceans during quality control, enabling quick identification of products with residual SO$_2$ concentrations above the legal limit. The label can also be used by end consumers to monitor product safety when a dark-blue test result would mean that the product is safe for consumption. For future works, the labels could be tested in other commercial temperatures and in different seafood products, as well as an indirect contact mode, aiming to expand their application.

5. Author's Contribution

- **Conceptualization** – Gleyca de Jesus Costa Fernandes; Marali Vilela Dias; Soraia Vilela Borges.

- **Data curation** – Gleyca de Jesus Costa Fernandes; Marali Vilela Dias.

- **Formal analysis** – Gleyca de Jesus Costa Fernandes; Pedro Henrique Campelo.

- **Investigation** – Gleyca de Jesus Costa Fernandes; Pedro Henrique Campelo; Beatriz Ribeiro Cabral.

- **Methodology** – Gleyca de Jesus Costa Fernandes; Marali Vilela Dias.

- **Project administration** – Marali Vilela Dias.

- **Resources** – Marali Vilela Dias; Soraia Vilela Borges; José Manoel Marconcini; Pedro Henrique Campelo; Zuy Maria Magriotis; Pedro Ivo Cunha Claro.

- **Software** – NA.

- **Supervision** – Marali Vilela Dias.

- **Validation** – Gleyca de Jesus Costa Fernandes; Marali Vilela Dias; Soraia Vilela Borges.

- **Visualization** – Karoline Ferreira Silva; Clara Suprani Marques; Luiza Zanini Benedito.

- **Writing – original draft** – Gleyca de Jesus Costa Fernandes.

- **Writing – review & editing** – Karoline Ferreira Silva; Clara Suprani Marques; Marali Vilela Dias; Luiza Zanini Benedito.

6. Acknowledgements

7. References

1. Sae-leaw, T., & Benjakul, S. (2019). Prevention of melanosis in crustaceans by plant polyphenols: a review. *Trends in Food Science & Technology*, *85*, 1-9. http://dx.doi.org/10.1016/j.tifs.2018.12.003.

2. Lien, K.-W., Hsieh, D. P. H., Huang, H.-Y., Wu, C.-H., Ni, S.-P., & Ling, M.-P. (2016). Food safety risk assessment for estimating dietary intake of sulfites in the Taiwanese population. *Toxicology Reports*, *3*, 544-551. http://dx.doi.org/10.1016/j.toxrep.2016.06.003. PMid:28959578.

3. Brasil. (2019, 19 de dezembro). *Resolução - RDC Nº 329 - Estabelece os aditivos alimentares e coadjuvantes de tecnologia autorizados para uso em pescado e produtos de pescado*. Diário Oficial da União, Brasília.

4. Andrade, L. T., Lacerda, M. F. A. F., & Ventura, A. P. M. (2015). Uso do dióxido de enxofre na despesca e beneficiamento de camarão. *Revista Principia Divulgação Científica e Tecnológica do IFPB*, *1*(28), 66-77. http://dx.doi.org/10.18265/1517-03062015v1n28p66-77.

5. D'Amore, T., Di Taranto, A., Berardi, G., Vita, V., Marchesani, G., Chiaravalle, A. E., & Iammarino, M. (2020). Sulfites in meat: occurrence, activity, toxicity, regulation, and detection. A comprehensive review. *Comprehensive Reviews in Food Science and Food Safety*, *19*(5), 2701-2720. http://dx.doi.org/10.1111/1541-4337.12607. PMid:33336981.

6. Bener, M., Şen, F. B., & Apak, R. (2020). Novel pararosaniline based optical sensor for the determination of sulfite in food extracts. *Spectrochimica Acta. Part A: Molecular and Biomolecular Spectroscopy*, *226*, 117643. http://dx.doi.org/10.1016/j.saa.2019.117643. PMid:31627056.

7. Mohammadian, E., Alizadeh-Sani, M., & Jafari, S. M. (2020). Smart monitoring of gas/temperature changes within food packaging based on natural colorants. *Comprehensive Reviews in Food Science and Food Safety*, *19*(6), 2885-2931. http://dx.doi.org/10.1111/1541-4337.12635. PMid:33337068.

8. Kalpana, S., Priyadarshini, S. R., Leena, M. M., Moses, J. A., & Anandharamakrishnan, C. (2019). Intelligent packaging: trends and applications in food systems. *Trends in Food Science & Technology*, *93*, 145-157. http://dx.doi.org/10.1016/j.tifs.2019.09.008.

9. Fu, L., Liu, C.-C., Yang, C., Wang, Y., & Ko, C. (2019). A PET/paper chip platform for high resolution sulphur dioxide detection in food. *Food Chemistry*, *286*, 316-321. http://dx.doi.org/10.1016/j.foodchem.2019.02.032. PMid:30827613.

10. Khamkhajorn, C., Pencharee, S., Jakmunee, J., & Youngvises, N. (2022). Smartphone-based colorimetric method for determining sulfites in wine using a universal clamp sample holder and microfluidic cotton swab-based analytical device. *Microchemical Journal*, *174*, 107055. http://dx.doi.org/10.1016/j.microc.2021.107055.

11. Csekõ, G., Varga, D., Horváth, A. K., & Nagypál, I. (2008). Simultaneous investigation of the Landolt and Dushman reactions. *The Journal of Physical Chemistry A*, *112*(26), 5954-5959. http://dx.doi.org/10.1021/jp802239b. PMid:18543894.

12. Fernandes, G. J. C. (2016). Desenvolvimento de etiqueta inteligente com indicador colorimétrico para identificação de SO2 em crustáceos (Dissertação de mestrado). Universidade Federal de Lavras, Lavras.

13. Wang, Y., Zhang, L., Liu, H., Yu, L., Simon, G. P., Zhang, N., & Chen, L. (2016). Relationship between morphologies and mechanical properties of hydroxypropyl methylcellulose/hydroxypropyl starch blends. *Carbohydrate Polymers*, *153*, 329-335. http://dx.doi.org/10.1016/j.carbpol.2016.07.029. PMid:27561503.

14. Salez, T., McGraw, J. D., Dalnoki-Veress, K., Raphaël, E., & Forrest, J. A. (2017). Glass transition at interfaces. *Europhysics News*, *48*(1), 24-28. http://dx.doi.org/10.1051/epn/2017103.

15. Luchese, C. L., Sperotto, N., Spada, J. C., & Tessaro, I. C. (2017). Effect of blueberry agro-industrial waste addition to corn starch-based films for the production of a pH-indicator film. *International Journal of Biological Macromolecules*, *104*(Pt A), 11-18. http://dx.doi.org/10.1016/j.ijbiomac.2017.05.149 PMid:28552729.

16. Vieira, K. P. B. A., Góes, L. M. N., Mendes, P. P., Galvez, A. O., & Mendes, E. S. (2008). Influência do aquecimento sobre diferentes métodos de titulação de SO2 residual em camarões *Litopenaeus vannamei* (Boone, 1931). *Acta Scientiarum. Animal Sciences*, *30*(1), 83-88.

17. American Society for Testing and Materials – ASTM. (2015). *ASTM D1746-15: standard test method for transparency of plastic sheeting*. USA: ASTM.

18. Abral, H., Basri, A., Muhammad, F., Fernando, Y., Hafizulhaq, F., Mahardika, M., Sugiarti, E., Sapuan, S. M., Ilyas, R. A., & Stephane, I. (2019). A simple method for improving the properties of the sago starch films prepared by using ultrasonication treatment. *Food Hydrocolloids*, *93*, 276-283. http://dx.doi.org/10.1016/j.foodhyd.2019.02.012.

19. Shivaraju, V. K., Appukuttan, S. V., & Kumar, S. K. S. (2019). The Influence of bound water on the FTIR characteristics of starch and starch nanocrystals obtained from selected natural sources. *Stärke*, *71*(5-6), 1700026.

20. Basiak, E., Lenart, A., & Debeaufort, F. (2017). Effect of starch type on the physico chemical properties of edible films. *International Journal of Biological Macromolecules*, *98*, 348-356. http://dx.doi.org/10.1016/j.ijbiomac.2017.01.122. PMid:28137462.

21. Colivet, J., & Carvalho, R. A. (2017). Hydrophilicity and physicochemical properties of chemically modified cassava starch films. *Industrial Crops and Products*, *95*, 599-607. http://dx.doi.org/10.1016/j.indcrop.2016.11.018.

22. Shah, U., Naqash, F., Gani, A., & Masoodi, F. A. (2016). Art and science behind modified starch edible films and coatings: a review. *Comprehensive Reviews in Food Science and Food Safety*, *15*(3), 568-580. http://dx.doi.org/10.1111/1541-4337.12197. PMid:33401817.

23. Pigłowska, M., Kurc, B., Rymaniak, Ł., Lijewski, P., & Fuć, P. (2020). Kinetics and thermodynamics of thermal degradation of different starches and estimation the OH group and H$_2$O content on the surface by TG/DTG-DTA. *Polymers*, *12*(2), 357. http://dx.doi.org/10.3390/polym12020357. PMid:32041286.

24. Danilovas, P. P., Rutkaite, R., & Zemaitaitis, A. (2014). Thermal degradation and stability of cationic starches and their complexes with iodine. *Carbohydrate Polymers*, *112*, 721-728. http://dx.doi.org/10.1016/j.carbpol.2014.06.038. PMid:25129801.

25. Chen, Y., Yang, Y., Liao, Q., Yang, W., Ma, W., Zhao, J., Zheng, X., Yang, Y., & Chen, R. (2016). Preparation, property of the complex of carboxymethyl chitosan grafted copolymer with iodine and application of it in cervical antibacterial biomembrane. *Materials Science and Engineering C*, *67*, 247-258. http://dx.doi.org/10.1016/j.msec.2016.05.027. PMid:27287120.

26. Aqlil, M., Nzenguet, A. M., Essamlali, Y., Snik, A., Larzek, M., & Zahouily, M. (2017). Graphene oxide filled lignin/starch polymer bionanocomposite: structural, physical, and mechanical studies. *Journal of Agricultural and Food Chemistry*, *65*(48), 10571-10581. http://dx.doi.org/10.1021/acs.jafc.7b04155. PMid:29113432.

27. Moulay, S. (2013). Molecular iodine/polymer complexes. *Journal of Polymer Engineering*, *33*(5), 389-443. http://dx.doi.org/10.1515/polyeng-2012-0122.

28. Ali, A., Ganie, S. A., & Mazumdar, N. (2018). A new study of iodine complexes of oxidized gum arabic: an interaction between iodine monochloride and aldehyde groups. *Carbohydrate Polymers*, *180*, 337-347. http://dx.doi.org/10.1016/j.carbpol.2017.10.005. PMid:29103513.

29. Fan, F., & Roos, Y. H. (2017). Glass transition-associated structural relaxations and applications of relaxation times in amorphous food solids: a review. *Food Engineering Reviews*, *9*(4), 257-270. http://dx.doi.org/10.1007/s12393-017-9166-6.

30. Ramos, E. M., & Gomide, L. A. M. (2007). *Avaliação da qualidade de carnes: fundamentos e metodologias*. Viçosa: Editora UFV.

31. Leung, A. M., & Braverman, L. E. (2014). Consequences of excess iodine. *Nature Reviews. Endocrinology*, *10*(3), 136-142. http://dx.doi.org/10.1038/nrendo.2013.251. PMid:24342882.